Civil Engineering Dimension, Vol. 21, No. 2, September 2019, 89-96 DOI: 10.9744/CED.21.2.89-96
ISSN 1410-9530 print / ISSN 1979-570X online

On the Derivation of Exact Solutions of a Tapered Cantilever Timoshenko Beam

Wong, F.T.[1*], Gunawan, J.[2], Agusta, K,[3], Herryanto[4], and Tanaya, L.S.[5]

Abstract: A tapered beam is a beam that has a linearly varying cross section. This paper presents an analytical derivation of the solutions to bending of a symmetric tapered cantilever Timoshenko beam subjected to a bending moment and a concentrated force at the free end and a uniformly-distributed load along the beam. The governing differential equations of the Timoshenko beam of a variable cross section are firstly derived from the principle of minimum potential energy. The differential equations are then solved to obtain the exact deflections and rotations along the beam. Formulas for computing the beam deflections and rotations at the free end are presented. Examples of application are given for the cases of a relatively slender beam and a deep beam. The present solutions can be useful for practical applications as well as for evaluating the accuracy of a numerical method

Keywords: Timoshenko beam; tapered beam; the principle of minimum potential energy; slender beam; deep beam.

Introduction

A tapered beam is a beam with a linearly varying cross section and hence has a straight center-line. It is within the larger class of non-prismatic beams, i.e. "a beam with curvilinear center-line and non-constant cross-section" [1]. It is commonly used in various engineering structures such as buildings and bridges to achieve more optimal use of the material and to satisfy architectural or esthetical needs. There are several approaches for modeling non-prismatic beams for structural analysis and design, that is [1, 2]:

- Using a modified prismatic beam model, i.e., Euler-Bernoulli or Timoshenko beam model with varying cross-sectional area and moment of inertia,
- Using a generalized non-prismatic beam theory such as that recently developed by Balduzzi et al. [1] and Auricchio et al. [2],
- Using 2D or 3D finite elements.

This paper deals with the first approach, in particular, the Timoshenko beam model.

[1] Department of Civil Engineering, Petra Christian University, Jl. Siwalankerto 121-131, Surabaya 60236, INDONESIA.
[2] PT Waringin Megah, Surabaya, INDONESIA.
[3] Benjamin Gideon and Associates, Surabaya, INDONESIA.
[4] PT. Archimetric, Surabaya, INDONESIA.
[5] PT. Teno Indonesia, Surabaya, INDONESIA.
*Corresponding author; email: wftjong@petra.ac.id

Note: Discussion is expected before November, 1st 2019, and will be published in the "Civil Engineering Dimension", volume 22, number 1, March 2020.

Received 17 June 2019; revised 12 September 2019; accepted 19 September 2019.

Several studies have been carried out to obtain analytical solutions of non-prismatic beams based on a modified Euler-Bernoulli or Timoshenko beam model. For example, Fertis and Keene [3] presented an elastic and inelastic bending analysis of non-prismatic beams using the so-called method of the equivalent prismatic system. The advantage of this approach is that the exact solution of a non-prismatic Euler Bernoulli beam model can be obtained with reduced mathematical complexity. Romano and Zingore [4] obtained analytical solutions of non-prismatic Euler-Bernoulli beams with a linearly and quadratically varying depth or with a linearly varying width of the rectangular cross section. The solutions were obtained by solving the fourth-order linear differential equation with variable coefficients that govern the beam bending. Romaro [5] then extended his previous study [4] to obtain analytical solutions of the same non-prismatic beams based on a modified Timoshenko beam model including the effects of tapering slope on shear stress distribution on the cross sections. The solutions were achieved by transforming the forth-order differential equation with variable coefficients into that with constant coefficients. Al-Gahtani and Khan [6] presented an exact analysis of non-prismatic Euler-Bernoulli beam model with end elastic supports. The boundary integral method was used in their study.

This paper presents the derivation of analytical solutions of the Timoshenko beam model of a symmetric tapered cantilever beam subjected to a bending moment and a concentrated force at the free end, and a uniformly-distributed load (Figure 1). The term 'symmetric' here means that the longitudinal tapered beam geometry has an axis of symmetry,

that is, the line passing through the cross section centroids. The effects of the tapering slope on the shear stress distribution along the beam is neglected. Thus, the model used is simpler than that considered in Romano [5] but is finer than the Euler-Bernoulli beam model [4].

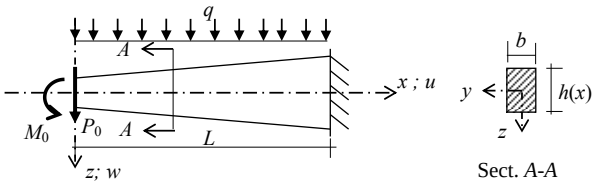

Figure 1. Tapered beam model

In the derivation, the differential equations governing bending of the beam is firstly derived from the total potential energy. The resulting differential equations are then analytically solved to obtain the exact solutions. For the sake of comparison and completeness, the solutions for the case of prismatic beams are also derived. Lastly, the solutions are applied to determine the deflections of a slender beam and a deep tapered beam with different tapering angles. In this example, the numerical solutions are compared to those obtained using the analytical solutions of Romano [5] and the finite element analysis of the plane stress model.

It is worth mentioning here that the use of the Timoshenko beam model to non-prismatic beams, in general, introduces a modeling error, which is proportional to the rate of cross section height variation [1,2]. However, due to its simplicity, it is still worthy of using this model in engineering practice to analyzed a symmetric tapered beam with a small tapering angle (i.e., a small rate of change in the height variation) [6,7]. For non-symmetric tapered beams, however, the modeling error may not be negligible even for a small tapering angle as can be seen in an example presented in Mercuri et al. [8]. The reason for this error is that the Timoshenko beam model neglects the coupling between bending and axial deformations occurred in non-symmetric tapered beams.

Governing Equations of the Tapered Beam Model

The beam under consideration is a tapered cantilever beam of the length L, as illustrated in Figure 1. The cross section is rectangular with the constant width b, and the height varies linearly from $h(0) = h_0$ at the left end to $h(L) = h_L = \alpha h_0$ at the right end, where $\alpha \geq 1$ (if $\alpha = 1$ then the beam is prismatic). The beam is made from a homogeneous, isotropic material with the modulus of elasticity E, Poisson's ration ν, and modulus of shear $G = E / (2(1+\nu))$. It is subjected to a bending moment M_0 and a concentrated load P_0 at the left end, and a uniform transversal load q (force/length) along the beam.

A right-handed Cartesian coordinate system x-y-z is set up with the point of origin O at the left end, as shown in Figure 1. According to the Timoshenko beam theory [9: p. 399], the displacement of a material point at coordinate (x, y, z) of the beam is;

$$u(x,y,z) = -z\theta(x)$$
$$w(x,y,z) = w(x) \tag{1}$$

where $u(x, y, z)$ and $w(x, y, z)$ are the displacement components of the material point in the x and z directions, respectively, $w(x)$ and $\theta(x)$ are the deflection (z-direction displacement) and rotation of the cross section at station x. The positive direction for $\theta(x)$ is the rotation from the x-axis to the z-axis (clockwise rotation).

A functional that governs the deformation of the beam is

$$\Pi[w,\theta] = U - W \tag{2a}$$
$$U = \tfrac{1}{2}\int_0^L EI\,\theta_{,x}^2\,dx + \tfrac{1}{2}\int_0^L GA_s(w_{,x} - \theta)^2\,dx \tag{2b}$$
$$W = -M_0\theta(0) + P_0 w(0) + \int_0^L qw\,dx \tag{2c}$$

where $\Pi[w, \theta]$ is the total potential energy of the beam, U is the elastic strain energy stored in the deformed beam, W is the potential work of the applied loads, I is the moment of inertia of the cross section about the y axis, and A_s is the effective shear area, i.e.

$$A_s = kA \tag{3a}$$

Commas followed by subscripts x indicate differentiation to x. In Equation (3a), A is the area of the cross section, and k is the shear coefficient. This coefficient is a correction factor needed to account for the difference between the assumed constant shear stress in the Timoshenko beam theory and the actual shear stress distribution. Cowper [10] presented a shear coefficient formula based on a derivation from the three-dimensional theory of elasticity, that is,

$$k = \frac{10(1+\nu)}{12+11\nu} \tag{3b}$$

for a rectangular cross section.

The deflection and rotation fields in the total potential energy, Equation (2), are required to be sufficiently regular and satisfy the essential boundary conditions. These requirements are written as follows:

$$w, \theta \in S = \{u | u \in H^1(0,L), u(L) = 0\} \tag{4a}$$

In this expression, S is the space of admissible solutions, $H^1(0, L)$ is the Hilbert function space (also

called the first Sobolev space) [11,12], which is defined as

$$\mathrm{H}^1(0,L) = \{u | \int_0^L (u^2 + L^2 u_{,x}^2)dx < \infty\} \quad (4b)$$

The principle of stationary potential energy [9: pp. 110-116, 13: pp. 137-140] for the beam can be written as

$$\delta\Pi = 0 \ \forall \ \delta w, \delta\theta \in \mathrm{V} = \{v | v \in \mathrm{H}^1, v(L) = 0\} \quad (5)$$

where δ is the variational operator, $\forall$ stands for 'for all', and V is the space of admissible displacement variations. Applying this principle to Equations (2) and (5) gives;

$$\int_0^L \delta\theta_{,x}\, EI\, \theta_{,x}\ dx + \int_0^L (\delta w_{,x} - \delta\theta) GA_\mathrm{s}(w_{,x} - \theta)dx + \delta\theta(0)M_0 - \delta w(0)P_0 - \int_0^L \delta w q\, dx = 0 \quad \forall\ \delta w, \delta\theta \in \mathrm{V} \quad (6)$$

Interpreting δw and $\delta\theta$ as the virtual deflection and virtual rotation, respectively, Equation (6) is recognized as of the principle of virtual displacement for the beam model.

Using integration by parts to the first and second terms of Equation (6), respectively, and using the requirements $\delta w(L) = \delta\theta(L) = 0$, these terms can be expressed as

$$\int_0^L \delta\theta_{,x}\, EI\, \theta_{,x}\ dx = -\int_0^L \delta\theta (EI\theta_{,x})_{,x}\, dx - \delta\theta(0)(EI\theta_{,x})]_{x=0} \quad (7a)$$

$$\int_0^L (\delta w_{,x} - \delta\theta) GA_\mathrm{s}(w_{,x} - \theta)dx = -\int_0^L \delta w\big(GA_\mathrm{s}(w_{,x} - \theta)\big)_{,x}\, dx - \delta w(0)\big(GA_\mathrm{s}(w_{,x} - \theta)\big)]_{x=0} - \int_0^L \delta\theta\, GA_\mathrm{s}(w_{,x} - \theta)dx \quad (7b)$$

Now, substituting these expressions into Equation (6) and arranging the resulting terms yields

$$-\int_0^L \delta\theta[(EI\theta_{,x})_{,x} + GA_\mathrm{s}(w_{,x} - \theta)]dx - \int_0^L \delta w\big[\big(GA_\mathrm{s}(w_{,x} - \theta)\big)_{,x} + q\big]dx - \delta\theta(0)\Big[(EI\theta_{,x})]_{x=0} - M_0\Big] - \delta w(0)\big[\big(GA_\mathrm{s}(w_{,x} - \theta)\big)]_{x=0} + P_0\big] = 0 \quad (8)$$

Since the variations, δw and $\delta\theta$, are completely arbitrary, except at x=L they must be zero, from Equation (8) one can extract a set of governing differential equations and boundary conditions as follows:

$$(EI\,\theta_{,x})_{,x} + GA_\mathrm{s}(w_{,x} - \theta) = 0 \quad \text{in } 0 < x < L \quad (9a)$$

$$\big(GA_\mathrm{s}(w_{,x} - \theta)\big)_{,x} + q = 0 \quad \text{in } 0 < x < L \quad (9b)$$

$$(EI\theta_{,x})]_{x=0} = M_0\ ;\ \big(GA_\mathrm{s}(w_{,x} - \theta)\big)]_{x=0} = -P_0 \quad (9c)$$

$$\theta(L) = 0\ ;\ w(L) = 0 \quad (9d)$$

Equation (9c) are the natural boundary conditions while Equation (9d) are the essential boundary conditions.

Note that the sign convention for the bending moment that consistent with the above derivation is positive when the upper longitudinal fibers are in tension (in contrast to the commonly used sign convention). For the shear force, it is positive when its direction is downward (follows the direction of the positive z axis) on the cross section with the normal vector pointing to the positive x axis.

Analytical Solutions of the Beam Governing Equations

The varying height, area, and moment of inertia of the beam cross sections can be expressed as follows:

$$h(x) = h_0(1 + ax)\ ,\ a = \frac{\alpha - 1}{L} \quad (10a)$$

$$A_\mathrm{s}(x) = A_{\mathrm{s}0}(1 + ax)\ ,\ A_{\mathrm{s}0} = kbh_0 \quad (10b)$$

$$I(x) = I_0(1 + ax)^3\ ,\ I_0 = \frac{bh_0^3}{12} \quad (10c)$$

Integrating Equation (9b) and imposing the shear force boundary condition, i.e., the second equation of Equation (9c), yield the shear force field

$$Q(x) = GA_\mathrm{s}(w_{,x} - \theta) = -qx - P_0 \quad (11)$$

Subsequently, substituting the shear force, Equation (11), into Equation (9a), integrating and imposing the moment boundary condition, i.e., the first equation of Equation (9c), yield the bending moment field

$$M(x) = EI\,\theta_{,x} = \frac{1}{2}qx^2 + P_0x + M_0 \quad (12)$$

These results, Equations (11) and (12), can be easily confirmed by using a simple static principle since the beam is statically determinate.

Now, substituting the varying moment of inertia, Equation (10c), into Equation (12) and dividing the result by EI_0 give

$$\theta_{,x} = \frac{q}{2EI_0}\frac{x^2}{(1+ax)^3} + \frac{P_0}{EI_0}\frac{x}{(1+ax)^3} + \frac{M_0}{EI_0}\frac{1}{(1+ax)^3} \quad (13)$$

Integrating Equation (13) (using the partial fraction technique for the first and second terms) yields

$$\theta(x) = \frac{q}{2EI_0}\Big(\frac{\ln(1+ax)}{a^3} + \frac{3+4ax}{2a^3(1+ax)^2}\Big) - \frac{P_0}{EI_0}\frac{1+2ax}{2a^2(1+ax)^2} - \frac{M_0}{EI_0}\frac{1}{2a(1+ax)^2} + C_\theta \quad (14)$$

where C_θ is an integration constant. Imposing the rotation boundary condition, i.e. the first equation of

Equation (9d), and substituting the resulting C_θ into Equation (14) yield the rotation field

$$\theta(x) = \frac{q}{4a^3EI_0}\left(2\ln\left(\frac{1+ax}{1+aL}\right) + \frac{3+4ax}{(1+ax)^2} - \frac{3+4aL}{(1+aL)^2}\right) - \frac{P_0}{2a^2EI_0}\left(\frac{1+2ax}{(1+ax)^2} - \frac{1+2aL}{(1+aL)^2}\right) - \frac{M_0}{2aEI_0}\left(\frac{1}{(1+ax)^2} - \frac{1}{(1+aL)^2}\right) \quad (15)$$

This solution is not applicable in the case of prismatic beams since $a = 0$ causes a division by zero. The solution for prismatic beams can be obtained by integrating Equation (13) with $a = 0$, the result of which is

$$\theta(x) = \frac{q}{6EI_0}(x^3 - L^3) + \frac{P_0}{2EI_0}(x^2 - L^2) + \frac{M_0}{EI_0}(x - L) \quad (16)$$

Dividing Equation (11) by GA_s, substituting A_s, Equation (10b), and placing $\theta(x)$ in the right hand side yield

$$w_{,x} = \theta - \frac{q}{GA_{s0}}\frac{x}{1+ax} - \frac{P_0}{GA_{s0}}\frac{1}{1+ax} \quad (17)$$

Substituting θ in Equation (17) by Equation (15) and integrating the equation (using the integration by parts for the first term of θ) give

$$w(x) = \frac{q}{4a^3EI_0}\left(\frac{2(1+ax)}{a}\ln\left(\frac{1+ax}{e(1+aL)}\right) + \frac{4}{a}\ln(1+ax) + \frac{1}{a(1+ax)} - \frac{3+4aL}{(1+aL)^2}x\right) - \frac{P_0}{2a^2EI_0}\left(\frac{2}{a}\ln(1+ax) + \frac{1}{a(1+ax)} - \frac{1+2aL}{(1+aL)^2}x\right) + \frac{M_0}{2aEI_0}\left(\frac{1}{a(1+ax)} + \frac{1}{(1+aL)^2}x\right) - \frac{q}{a^2GA_{s0}}(ax - \ln(1+ax)) - \frac{P_0}{aGA_{s0}}\ln(1+ax) + C_w \quad (18)$$

where $e = 2.71828\ldots$ is the Euler number and C_w is an integration constant. Imposing the deflection boundary condition, i.e. the second equation of Equation (9d), and substituting the resulting C_w into Equation (18), yield the deflection field

$$w(x) = w_{bq}(x) + w_{sq}(x) + w_{bP}(x) + w_{sP}(x) + w_{bM}(x) \quad (19a)$$

$$w_{bq}(x) = \frac{q}{4a^3EI_0}\left(\frac{2(1+ax)}{a}\ln\left(\frac{1+ax}{e(1+aL)}\right) + \frac{2(1+aL)}{a} + \frac{4}{a}\ln\left(\frac{1+ax}{1+aL}\right) + \frac{1}{a(1+ax)} - \frac{1}{a(1+aL)} - \frac{3+4aL}{(1+aL)^2}(x-L)\right) \quad (19b)$$

$$w_{sq}(x) = -\frac{q}{a^2GA_{s0}}\left(a(x-L) - \ln\left(\frac{1+ax}{1+aL}\right)\right) \quad (19c)$$

$$w_{bP}(x) = -\frac{P_0}{2a^2EI_0}\left(\frac{2}{a}\ln\left(\frac{1+ax}{1+aL}\right) + \frac{1}{a(1+ax)} - \frac{1}{a(1+aL)} - \frac{1+2aL}{(1+aL)^2}(x-L)\right) \quad (19d)$$

$$w_{sP}(x) = -\frac{P_0}{aGA_{s0}}\ln\left(\frac{1+ax}{1+aL}\right) \quad (19e)$$

$$w_{bM}(x) = \frac{M_0}{2aEI_0}\left(\frac{1}{a(1+ax)} - \frac{1}{a(1+aL)} + \frac{1}{(1+aL)^2}(x-L)\right) \quad (19f)$$

Here, w_{bq} and w_{sq} are the bending and shear contributions to the deflection due to the distributed load q, respectively; w_{bP} and w_{sP} are the bending and shear contributions to the deflection due to the point load P_0, respectively; and w_{bM} is the deflection due to the moment M_0.

The deflection field for prismatic beams can be obtained by substituting θ in Equation (17) by Equation (16), integrating the equation with setting $a = 0$, and imposing the deflection boundary condition. The result is

$$w(x) = w_{bq}(x) + w_{sq}(x) + w_{bP}(x) + w_{sP}(x) + w_{bM}(x) \quad (20a)$$

$$w_{bq}(x) = \frac{q}{6EI_0}\left(\frac{1}{4}x^4 - L^3x + \frac{3}{4}L^4\right);\ w_{sq}(x) = -\frac{q}{2GA_{s0}}(x^2 - L^2) \quad (20b)$$

$$w_{bP}(x) = \frac{P_0}{2EI_0}\left(\frac{1}{3}x^3 - L^2x + \frac{2}{3}L^3\right);\ w_{sP}(x) = -\frac{P_0}{GA_{s0}}(x - L) \quad (20c)$$

$$w_{bM}(x) = \frac{M_0}{EI_0}\left(\frac{1}{2}x^2 - Lx + \frac{1}{2}L^2\right) \quad (20d)$$

The deflection and rotation at the free end can be obtained by substituting for $x = 0$ into Equation (19) and Equation (15) for the case of tapered beams and into Equation (20) and Equation (16) for the case of prismatic beams, respectively. The results are, after simplifying and substituting for $\alpha = 1+aL$, presented in Tables 1-4.

Table 1. Tip Deflections of the Tapered Cantilever Beam Subjected to M_0, P_0, and q

Load	Component	
	Bending	Shear
M_0	$\frac{M_0L^2}{2EI_0\alpha^2}$	N.A.
P_0	$\frac{P_0}{2a^2EI_0}\left(\frac{2}{a}\ln\alpha - \frac{3\alpha-1}{\alpha^2}L\right)$	$\frac{P_0}{aGA_{s0}}\ln\alpha$
q	$\frac{q}{4a^3EI_0}\left(\frac{2\alpha^2-1}{a\alpha} - \frac{6\ln\alpha+1}{a} + \frac{4\alpha-1}{\alpha^2}L\right)$	$\frac{q}{a^2GA_{s0}}(aL - \ln\alpha)$

Table 2. Tip Rotations of the Tapered Cantilever Beam Subjected to M_0, P_0, and q

Load	Rotation
M_0	$-\frac{M_0L}{EI_0}\frac{\alpha+1}{2\alpha^2}$
P_0	$-\frac{P_0L^2}{2EI_0\alpha^2}$
q	$\frac{q}{4a^3EI_0}\left(3 - 2\ln\alpha - \frac{4\alpha-1}{\alpha^2}\right)$

Table 3. Tip Deflections of the Prismatic Cantilever Beam Subjected to M_0, P_0, and q

Load	Component	
	Bending	Shear
M_0	$\frac{M_0 L^2}{2EI_0}$	N.A.
P_0	$\frac{P_0 L^3}{3EI_0}$	$\frac{P_0 L}{GA_{s0}}$
q	$\frac{qL^4}{8EI_0}$	$\frac{qL^2}{2GA_{s0}}$

Table 4. Tip Rotations of the Prismatic Cantilever Beam Subjected to M_0, P_0, and q

	Rotation
M_0	$-\frac{M_0 L}{EI_0}$
P_0	$-\frac{P_0 L^2}{2EI_0}$
q	$-\frac{qL^3}{6EI_0}$

Remarks

1. Since the deflection and rotation for the case of tapered beams should converge to those of prismatic beams when the coefficient a approaches 0, the results in Tables 3 and 4 can be obtained by taking the limit of the corresponding results in Tables 1 and 2 as the coefficient a approaches 0. This is obvious when the coefficient $a = 0$ in Tables 1 or 2 does not cause a division by zero. For the other results, however, one should perform a limit calculation. For example, according to Table 1, the shear deflection due to P_0 is

$$w_{sP}(0) = \frac{P_0}{aGA_{s0}} \ln \alpha = \frac{P_0}{aGA_{s0}} \ln(1 + aL) \tag{21}$$

Taking the limit as a approaches 0 and applying the l'Hospital rule,

$$w_{sP}(0) = \lim_{a \to 0} \frac{P_0}{aGA_{s0}} \ln(1 + aL) \tag{22a}$$

$$w_{sP}(0) = \frac{P_0}{GA_{s0}} \lim_{a \to 0} \frac{\ln(1+aL)}{a} = \frac{P_0}{GA_{s0}} \lim_{a \to 0} \frac{L}{1+aL} = \frac{P_0 L}{GA_{s0}} \tag{22b}$$

This result is identical to the shear deflection of the prismatic beam due to P_0 given in Table 3. The convergence of the tapered beam solutions towards prismatic beam solutions as the coefficient a approaches zero will also be demonstrated in the following numerical examples.

2. Equation (15) and (16) and also Tables 2 and 4 show that there is no contribution of the shear deformation to the cross section rotations. Therefore, the rotation formulas are the same as those given by the classical Euler-Bernoulli beam theory. For example, the prismatic beam displacement table in Ghali and Neville [14] gives the same results for the free end rotation as those given in Table 4.
3. The bending contribution to the tip deflections of prismatic beams due to M_0, P_0, and q (Table 3) are the same as the tip deflection given by the classical beam theory presented in Ghali and Neville [14].
4. For a given constant h_0, as the beam becomes very slender, i.e., as $L \to \infty$, the beam approaches the prismatic beam, i.e., $a \to 0$. From Table 3, it is evident that for very slender beam the deflection is dominated by the bending contribution and hence the deflections converge to the classical Euler-Bernoulli deflections.

Examples of Application

Consider symmetric cantilever beams of the slenderness ratios $L/h_L = 10$ (a relatively slender beam) and $L/h_L = 2.5$ (a deep beam). The lengths of the beams are $L = 4$ m and $L = 1$ m for the slender and deep ones, respectively. The height at the fixed end is $h_L = 0.4$ m; the width is $b = 0.2$ m. For the present parametric study, the end-thickness ratios $\alpha = h_1/h_0$ are varied from 1 (prismatic beam), 1.5, 2, and 3. Figure 2 illustrates the slender beam vs. the deep beam for $\alpha = 2$. Table 5 summarizes the geometric parameters of the eight different cases considered. In this table, φ is the inclination angle of the top or bottom faces of the beam (tapering angle). The material properties are $E = 20000$ MPa and $\nu = 0.2$, which are typical properties of normal concrete. The loads are taken as follows: $M_0 = 10$ kN-m, $P_0 = 10$ kN, and $q = 10$ kN/m for the slender beam and $q = 40$ kN/m for the deep beam (the total load is taken to be equal, that is, 40 kN).

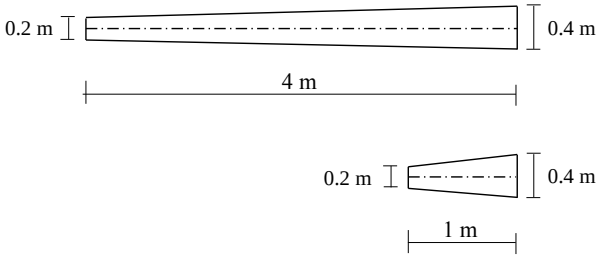

Figure 2. Symmetrically Tapered Beams with the end-Thickness Ratios $\alpha = 2$ (scaled): (a) Slender Beam, (b) Deep Beam

Table 5. Geometric Parameters used in the Case Study

L (m)	α	h_L (m)	h_0 (m)	α (/m)	φ (deg)
4	1	0.400	0.400	0	0.00
4	1.5	0.400	0.267	0.125	0.95
4	2	0.400	0.200	0.25	1.43
4	3	0.400	0.133	0.5	1.91
1	1	0.400	0.400	0	0.00
1	1.5	0.400	0.267	0.5	3.80
1	2	0.400	0.200	1	5.65
1	3	0.400	0.133	2	7.47

Numerical Results

Deflections of the slender beam and deep beam due to end moment M_0 for different cases of end-height ratios α are presented in Figures 3 and 4, respectively, due to end concentrated load P_0 in Figures 5 and 6, respectively, and due to distributed load q in Figures 7 and 8, respectively. It is seen that the deflections of the slender beam are, as expected, much larger than those of the deep beam. The tip deflections of the slender beam subjected to M_0 are 16 times larger, while those subjected to P_0 and q (with equal total load) are about 56 to 60 times larger. As also expected, the thinner the cross-section at the free end (or the larger the end-thickness ratios α), the larger the deflections. For the beams subjected to M_0, the tip deflections become twice larger when the free-end cross sections are twice thinner. While for the beams subjected to P_0 and q, the tip deflections are about 1.6 and 1.4 times larger, respectively when the free-end cross sections are twice thinner.

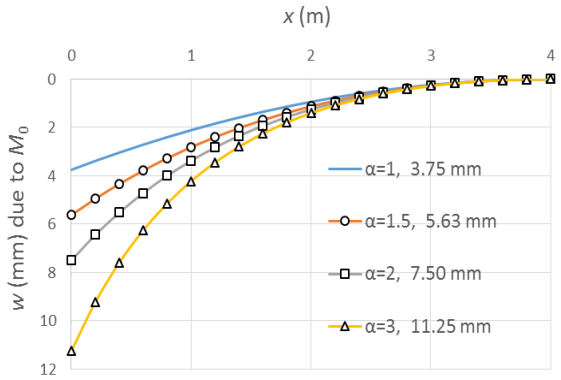

Figure 3. Deflection of the Beam of Length 4 m Subjected to M_0 = 10 kN-m for Different Values of End Height Ratios α. Values in the Legend Indicate the Deflection at the Left End.

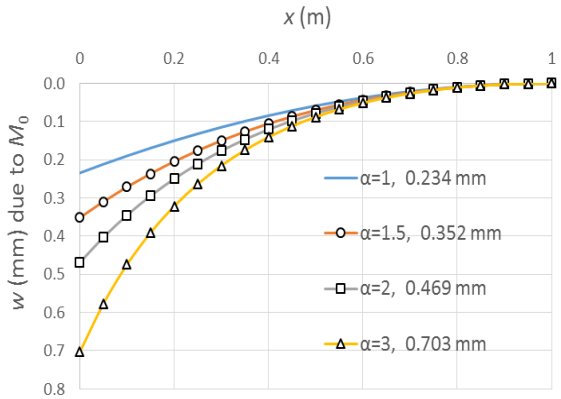

Figure 4. Deflection of the Beam of Length 1m Subjected to M_0 = 10 kN-m for Different Values of End Height Ratios α. Values in the Legend Indicate the Deflection at the Left End.

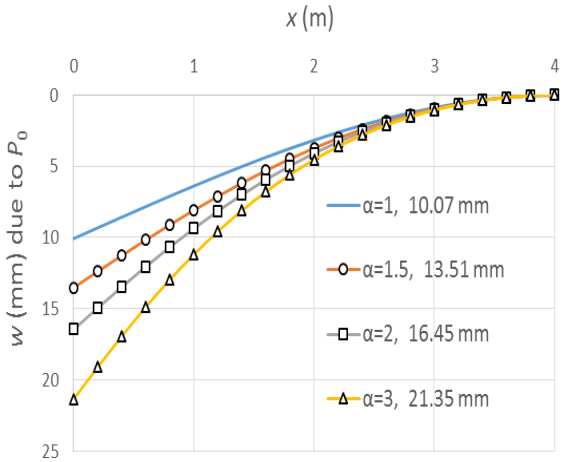

Figure 5. Deflection of the Beam of Length 4 m Subjected to P_0 for Different Values of end Height Ratios α. Values in the Legend Indicate the Deflection at the Left End.

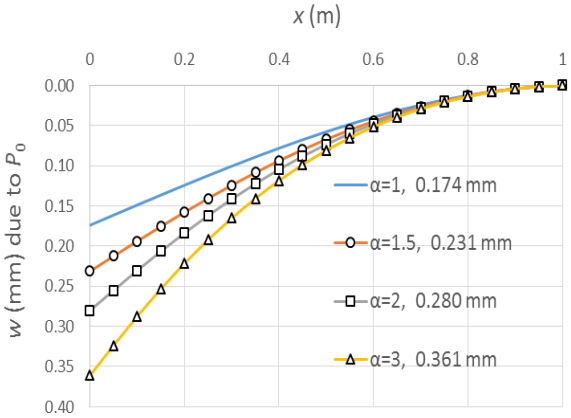

Figure 6. Deflection of the Beam of Length 1 m Subjected to P_0 = 10 kN for Different Values of end Height Ratios α. Values in the Legend Indicate the Deflection at the Left End.

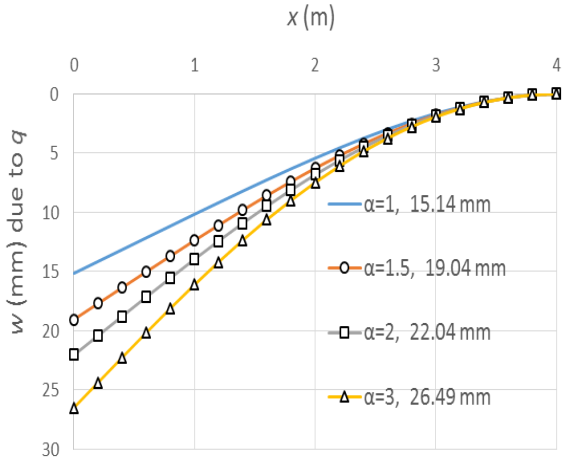

Figure 7. Deflection of the Beam of Length 4 m Subjected to q = 10 kN/m for Different Values of end Height Ratios α. Values in the Legend Indicate the Deflection at the Left End.

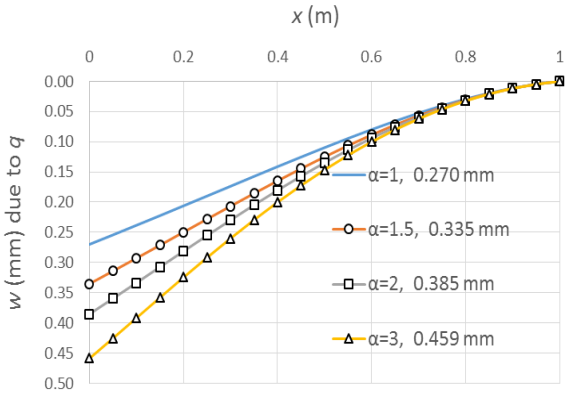

Figure 8. Deflection of the Beam of Length 1 m Subjected to q = 40 kN/m for Different Values of End Height Ratios α. Values in the Legend Indicate the Deflection at the Left End.

Contribution of Shear Deformation

For the beams subjected to end moment M_0, it is evident from Equations (19f) and (20d) and from Tables 1 and 3 that there is no contribution of shear deformation to the deflections. Contribution of shear deformation to the tip deflections for the beams subjected to concentrated load P_0 and q is presented in Table 6. The contribution of shear deformation for the slender beams (L/h_L = 10) is, as expected, practically insignificant. While for the deep beams (L/h_L = 2.5), the contribution of shear deformation cannot be neglected. It is seen that the contribution of shear deformation multiplies about 14 to 15 times when the slenderness, L/h_L, decreases four times (that is, from L/h_L = 10 to L/h_L = 2.5). This in agreement with the fact that the upper bound of the shear deformation contribution is proportional to the square of L/h_L, which is 16 for this case.

Table 6. Percentages of Shear Deformation Contribution to the Tip Deflections of Slender and Deep Beams Subjected to P_0 and q

α	P_0		q	
	L = 4 m	L = 1 m	L = 4 m	L = 1 m
1	0.70%	10.20%	0.94%	13.15%
1.5	0.64%	9.33%	0.85%	12.01%
2	0.60%	8.78%	0.79%	11.31%
3	0.55%	8.10%	0.72%	10.46%

Convergence towards Prismatic Beams

To study the convergence of the deflection solutions of tapered beams, Equation (19), towards the solutions of the prismatic beam, Equation (20), the values of the tip deflections, Table 1, are numerically examined as the values of α approaches 1 (that is, equivalent to coefficient α approaches 0). Tables 7 and 8 present the tip deflections for the cases of the slender and deep beams, respectively. It is seen that, as expected, all of the solutions of the tapered beams converge well towards the solutions of the prismatic beams as α approaches 1.

Table 7. Tip Deflections of the Tapered Cantilever Beam as $\alpha \rightarrow 1$ for the Case of L = 4 m

α	$w_{bM}(0)$	$w_{bP}(0)$	$w_{sP}(0)$	$w_{bq}(0)$	$w_{sq}(0)$
1.5	5.625	13.43	8.636E-02	18.88	0.1611
1.2	4.500	11.44	7.767E-02	16.69	0.1506
1.1	4.125	10.74	7.444E-02	15.87	0.1465
1.05	3.938	10.37	7.275E-02	15.44	0.1443
1.01	3.788	10.07	7.135E-02	15.09	0.1425
1.001	3.754	10.01	7.104E-02	15.00	0.1420
1	3.750	10.00	7.100E-02	15.00	0.1420

Table 8. Tip Deflections of the Tapered Cantilever Beam as $\alpha \rightarrow 1$ for the Case of L = 1 m

α	$w_{bM}(0)$	$w_{bP}(0)$	$w_{sP}(0)$	$w_{bq}(0)$	$w_{sq}(0)$
1.5	0.3516	0.2098	2.159E-02	0.2950	4.027E-02
1.2	0.2813	0.1788	1.942E-02	0.2608	3.766E-02
1.1	0.2578	0.1677	1.861E-02	0.2480	3.663E-02
1.05	0.2461	0.1621	1.819E-02	0.2413	3.608E-02
1.01	0.2367	0.1574	1.784E-02	0.2358	3.562E-02
1.001	0.2346	0.1564	1.776E-02	0.2344	3.551E-02
1	0.2344	0.1563	1.775E-02	0.2344	3.550E-02

Comparison with the Solutions of Other Beam Models

To assess the validity of the present Timoshenko beam model, the tip deflections at the free end for the case of the beams with the height ratio of α = 2 (see Figures 3-8) are compared to the solutions based on the beam model presented by Romano [5] and the plane stress model (Table 9). The tip deflections of Romano [5] were obtained by applying the analytical solution of Romano [5] to the cantilever beam considered in this paper, that is,

$$w(x) = C_1 + C_2 \ln(h_0 + ax) + C_3(h_0 + ax) + \frac{C_4}{h_0 + ax}$$

$$+R_1(h_0 + ax)\ln(h_0 + ax) \qquad (23a)$$

$$R_1 = \frac{6q}{(h_0 a)^4 Eb} \qquad (23b)$$

where C_1, C_2, C_3, and C_4 are integration constants that were determined from the boundary conditions: $Q(0) = -P_0$; $M(0) = -M_0$ (following the sign convention in Romano [5]); $w(L) = 0$; $\theta(L) = 0$. While, the tip deflections of the plane stress model were obtained from finite element analyses using the mesh of 160×8 and 80×16 quadrilateral elements for the beam of the slenderness ratio L/h = 10 and L/h = 2.5, respectively. The element used was the four-node quadrilateral element including bending incompatible modes contained in software SAP2000 [15].

Table 9. Tip Deflections (mm) of the Tapered Cantilever Beams for α = 2

Load case	Slenderness ratio	Present	Romano [5]	Plane stress
M_0	L/h = 10	7.50	7.43	7.49
	L/h = 2.5	0.469	0.401	0.465
P_0	L/h = 10	16.45	16.51	16.43
	L/h = 2.5	0.280	0.294	0.276
q	L/h = 10	22.04	22.01	22.00
	L/h = 2.5	0.385	0.376	0.379

The table shows that for the slender beam of L/h = 10, there is no significant difference among the results obtained using different models (the difference among the results is less than 1%). For the deep beam of L/h = 2.5 subjected to moment M_0 and concentrated load P_0, the present solutions are closer to the plane stress results than those of Romano [5]. For the deep beam subjected to distributed load q, however, Romano's solutions are closer. The overall results of this comparison demonstrate the validity of the present beam model.

Conclusions

Exact solutions of the Timoshenko beam model for cantilever tapered and prismatic beams subjected to an end moment, an end concentrated force, and a uniformly distributed force have been derived by solving the governing differential equations. The solutions include the shear force and bending moment distributions, which are in agreement with the static principle, as well as the rotation and deflection fields. Based on these solutions, the formulas for computing the tip deflections and rotations have been presented. The numerical examples demonstrate the validity of the present solutions. The solutions and formulas may be useful for evaluating a numerical method such as Timoshenko beam finite elements [16,17], as well as for evaluating the deflection of a tapered cantilever beam in real engineering practice.

References

1. Balduzzi, G., Aminbaghai, M., Sacco, E., Füssl, J., Eberhardsteiner, J., and Auricchio, F., Non-prismatic Beams : A Simple and Effective Timoshenko-like Model, *International Journal of Solids and Structures*, Elsevier, 90, 2016, pp. 236–250.
2. Auricchio, F., Balduzzi, G., and Lovadina, C., The Dimensional Reduction Approach for 2D Non-prismatic Beam Modelling : A Solution based on Hellinger–Reissner Principle, *International Journal of Solids and Structures*, Elsevier, 63, 2015, pp. 264–276.
3. Fertis, D.G. and Keene, M.E., Elastic and inelastic Analysis of Nonprismatic Members, *Journal of Structural Engineering*, ASCE, 116(2), 1990, pp. 475–489.
4. Romano, F. and Zingone, G., Deflections of Beams with Varying Reactangular Cross Section, *Journal of Engineering Mechanics*, ASCE, 118(10), 1992, pp. 2128–2134.
5. Romano, F., Deflections of Timoshenko Beam with Varying Cross-Section, *International Journal of Mechanical Sciences*, Elsevier, 38(84), 1996, pp. 1017–1035.
6. Al-Gahtani, H.J. and Khan, M.S., Exact Analysis of Nonprismatic Beams, *Journal of Engineering Mechanics*, ASCE, 124(11), 1998, pp. 1290–1293.
7. Boley, B.A., On the Accuracy of the Bernoulli-Euler Theory for Beams of Variable Section, *Journal of Applied Mechanics*, ASME, 30(3), 1963, pp. 373–378.
8. Mercuri, V., Balduzzi, G., Asprone, D. and Auricchio, F., 2D Non-prismatic Beam Model for Stiffness Matrix Evaluation, *Proceedings of the World Conference on Timber Engineering*, Vienna, Austria, August 22-25, 2016.
9. Bathe, K. J., *Finite Element Procedures*, Prentice-Hall, New Jersey, 1996.
10. Cowper, G.R., The Shear Coefficient in Timoshenko's Beam Theory, *Journal of Applied Mechanics*, ASME, 33(2), 1966, pp. 335–340.
11. Hughes, T.J.R., *The Finite Element Method: Linear Static and Dynamic Finite Element Analysis*, Prentice-Hall, New Jersey,1987.
12. Garikipati, K., Introduction to Finite Element Methods, *Open Michigan*, 2013. Available: https://open.umich.edu/find/open-educational-resources/engineering/introduction-finite-element-methods. [Accessed: 23-Jan-2019].
13. Cook, R.D., Malkus, D.S., Plesha, M.E. and Witt, R.J., *Concepts and Applications of Finite Element Analysis*, Fourth edition, John Wiley and Sons, New York, 2002.
14. Ghali, A. and Neville, A., *Structural Analysis: A Unified Classical and Matrix Approach*, Second edition, Chapman and Hall, London, 1978.
15. *CSI Analysis Reference Manual for SAP2000, ETABS, and SAFE*, Computers and Structures Berkeley, California, 1995.
16. Wong, F.T. and Sugianto, S., Study of the Discrete Shear Gap Technique in Timoshenko Beam Elements, *Civil Engineering Dimension*, Petra Christian University, 19(1), 2017, pp. 54–62.
17. Wong, F.T., Sulistio, A., and Syamsoeyadi, H., Kriging-Based Timoshenko Beam Elements with the Discrete Shear Gap Technique, *International Journal of Computational Methods*, World Scientific, 15(07), 2018, pp. 1850064-1–1850064-27.